



Effects of polymer addition on the non-strongly interacting binary co-amorphous system carvedilol-tryptophan

Yixuan Wang, Holger Grohganz^{*}, Thomas Rades

Department of Pharmacy, University of Copenhagen, Universitetsparken 2, 2100 Copenhagen, Denmark

ARTICLE INFO

Keywords:

Polymer
Amorphization
Poorly water-soluble drugs
Molecular interaction
Dissolution
Physical stability

ABSTRACT

Co-amorphous systems have been developed to address the solubility challenge of poorly water-soluble crystalline drugs. However, due to the thermodynamic instability of amorphous forms, amorphization may result in recrystallization during manufacturing, storage, or dissolution, which is one of the main challenges in the pharmaceutical development of amorphous systems. This could also be the case in some co-amorphous systems with only non-strong interactions between the drug and the co-former (such as hydrogen bond formation and π - π interactions). In this study, a small amount of polymer was added to the binary co-amorphous mixture carvedilol (CAR) - tryptophan (TRP) at a molar ratio of 1:1 and subjected to mechanical activation by ball milling to produce amorphous systems, in order to investigate the effect of co-formulated polymer on the physical properties (solubility, stability, etc.) of non-strongly interacting binary co-amorphous mixtures. After co-formulating polymer to the binary co-amorphous system, stronger interactions were found between CAR and polymer than between CAR and TRP in the ternary polymer containing co-amorphous systems. Compared to the corresponding binary co-amorphous systems, larger areas under the dissolution curves were achieved, indicating an improvement in dissolution behaviour due to a more gradual increase in dissolved drug concentration and a longer period of maintaining drug supersaturation. There was no negative effect of polymer addition on physical stability at room temperature under dry storage conditions for 6 months. Therefore, it is possible to design ternary co-amorphous drug delivery systems with optimized dissolution characteristics by adding a small amount of polymer into co-amorphous binary systems.

1. Introduction

Solid dosage forms are widely used in oral drug delivery *inter alia* because of their good long-term chemical drug stability and versatility to modify drug release in pharmaceutical development (Carstensen and Pharmacy, 1988; Hirani et al., 2009). However, due to the absorption process of orally administered drugs, there are also some limitations. Many drugs do not have a sufficiently high dissolution rate and solubility in the fluids of the gastrointestinal tract, resulting in low bioavailability (Tang et al., 2008) and even low therapeutic efficacy (Tița et al., 2011). In order to address the poor water solubility challenge of many drug candidates, amorphous, rather than crystalline, forms of drugs have been developed and are considered an important emerging tool to increase drug water solubility (Wu et al., 2019). Compared with the corresponding crystalline forms, drugs in the amorphous form are characterized by long-range disorder, although they may still show some short-range order (An et al., 2020). Amorphous forms have higher free

energy than their crystalline counterparts, their particle surface is easier to hydrate, and thus drug molecules are more easily dispersed from the solid form (Wei et al., 2018), thereby improving the apparent solubility and the dissolution rate (which in the case of an amorphous material *stricto sensu* is a dilution) of poorly water-soluble drugs (Hancock and Zografi, 1997). However, the amorphous form is thermodynamically unstable, and thus most amorphous drugs show low physical stability and an inherent tendency to re-crystallize to their respective crystalline forms during manufacture, storage, or administration. This makes the use of pure amorphous drugs a challenge in practical applications (Di et al., 2021).

Based on the instability of amorphous drugs and the promising concept of using single-phase amorphous binary systems (such as amorphous solid dispersions) (Guo et al., 2014a), co-amorphous systems, as a new drug containing amorphous solid form, have emerged to address the poor physical stability of pure amorphous drugs and the low aqueous solubility of pure crystalline drugs (Dengale et al., 2016). Co-

^{*} Corresponding author.

E-mail address: holger.grohganz@sund.ku.dk (H. Grohganz).

<https://doi.org/10.1016/j.ijpharm.2022.121625>

Received 3 January 2022; Received in revised form 23 February 2022; Accepted 25 February 2022

Available online 5 March 2022

0378-5173/© 2022 The Authors. Published by Elsevier B.V. This is an open access article under the CC BY license (<http://creativecommons.org/licenses/by/4.0/>).

Table 1

Compositions of the physical mixtures used to prepare the single, binary and ternary system samples for solid state characterization, the dissolution and the stability study.

	Samples (superscript indicates for which part of the study the samples were used)	Content (W/W)			Molar ratio of CAR to TRP (mol/mol)
		CAR	TRP	Polymer (HPMC or PVPVA64)	
Single amorphous components	CAR ^{SST, DIS, STA}	100%	–	–	–
	TRP ^{SST}	–	100%	–	–
	Polymer (HPMC/PVPVA64) ^{SST}	–	–	100%	–
Binary co-amorphous systems	TRP-polymer (10% w/w) ^{SST}	–	90.9%	9.1%	–
	CAR-polymer (10% w/w) ^{SST, STA}	90.9%	–	9.1%	–
	CAR-TRP 1:1 ^{SST, DIS*}	66.5%	33.5%	–	1:1
Ternary co-amorphous system	CAR (66.5% w/w)-polymer ^{DIS}	66.5%	–	33.5%	–
	CAR-TRP 1.38:1-polymer (10% w/w) ^{DIS **}	66.5%	24.4%	9.1%	1.38:1
	CAR-TRP 1:1-polymer (1% w/w) ^{STA}	65.9%	33.1%	1%	1:1
	CAR-TRP 1:1-polymer (2% w/w) ^{STA}	65.2%	32.8%	2%	1:1
	CAR-TRP 1:1-polymer (3% w/w) ^{STA}	64.6%	32.5%	2.9%	1:1
	CAR-TRP 1:1-polymer (4% w/w) ^{STA}	64.0%	32.2%	3.5%	1:1
	CAR-TRP 1:1-polymer (5% w/w) ^{STA}	63.4%	31.8%	4.8%	1:1
	CAR-TRP 1:1-polymer (10% w/w) ^{SST, DIS, STA}	60.5%	30.4%	9.1%	1:1

The percentage in parenthesis stands for added polymer relative to other ingredients. SST stands for solid state characterization, DIS for dissolution and STA for stability study.

*When the molar ratio of CAR-TRP binary co-amorphous system is 1:1, the content of the system is 66.5% CAR and 33.5% TRP.

**When the molar ratio of CAR to TRP in CAR-TRP-polymer (10% w/w) ternary co-amorphous system is 1.38:1, the content of the system is 66.5% of CAR, 24.4% of TRP and 9.1% of polymer.

amorphous systems are single-phase amorphous binary systems containing the drug and a low molecular weight co-former. They can be divided into two categories according to the different kinds of molecular interactions between drug and co-former. One category shows strong interactions (such as ionic interactions), and the other shows non-strong interactions (such as hydrogen bond formation and π - π interactions) between the drug and the co-former. Both, non-strong and strong molecular interactions in these co-amorphous systems can play a crucial role in physical stabilization of the amorphous systems as well as in the dissolution and solubility enhancement of the drug. Additionally, the combination of two drugs (where one acts as the co-former for the other) can produce a synergistic pharmacological effect, thereby improving clinical efficacy and potentially reducing side effects of drugs (Kargianni et al., 2018). Therefore, co-amorphous systems may be of great significance for the dosage form design of poorly water-soluble drugs, and several studies have successfully demonstrated their advantages as solid pharmaceutical dosage forms (Fucke et al., 2012; Huang et al.,

2017; Löbmann et al., 2012).

However, there are still some challenges for the wider application of the co-amorphization concept. In some cases, the rapid initial dissolution rate of co-amorphous formulations may lead to very high supersaturation and rapid drug precipitation, thereby rendering co-amorphous formulations lose their dissolution advantages, e.g. in the fluids of the gastrointestinal tract (Laitinen et al., 2017; Xie et al., 2017). Therefore, a small amount of polymer has been added into co-amorphous systems to design ternary co-amorphous drug delivery systems with optimized dissolution characteristics. The additional polymer can modulate the drug release rate and maintain drug supersaturation by acting as a crystallization inhibitor (Liu et al., 2020a; Warren et al., 2010; Xie et al., 2017).

Our previous study by Liu et al. has indicated that adding polymer to the strongly interacting co-amorphous system carvedilol-L-aspartic acid (forming a co-amorphous salt) could improve the dissolution behaviour of the drug by reducing the extremely fast initial drug dissolution rate and maintaining supersaturation for a longer period (Liu et al., 2020a). Amorphous salt formation was in this case not interfered with by the added polymer. However, the influence of polymer addition on non-strongly interacting co-amorphous systems is not well known and will therefore be investigated in this study. To ensure the continuity of research, the drug carvedilol was again used in this study together with the amino acid L-tryptophan as model drug and co-former, respectively (Di et al., 2021). Two commonly used pharmaceutically relevant polymers, hydroxypropyl methylcellulose (HPMC) and poly-(vinylpyrrolidone-co-vinyl acetate) (PVPVA64), were co-formulated with the CAR-TRP co-amorphous mixtures in order to explore the effects of additional polymer on the physical properties (intermolecular interaction, dissolution enhancement, and stability) of the non-strongly interacting binary co-amorphous system.

2. Materials and methods

2.1. Materials

Carvedilol (CAR, MW = 406.47 g/mol) was purchased from Cipla Ltd. (Mumbai, India); L-tryptophan (TRP, MW = 204.23 g/mol) was used as the co-former and was purchased from Sigma-Aldrich (St. Louis, MO, USA). HPMC (Pharmacoat 603, substitution type 2910, viscosity 3 mPas) was purchased from Shin-Etsu Chemicals Co. (Chiyoda-ku, Tokyo, Japan); PVPVA64 (Kollidon VA 64 Fine) was purchased from BASF North America (Florham Park, New Jersey, USA).

2.2. Methods

2.2.1. Preparation of single component, binary, and ternary amorphous systems by ball milling

In order to compare CAR-TRP-polymer ternary systems with their corresponding single and binary systems samples, CAR, TRP, polymer, CAR-TRP, CAR-polymer, TRP-polymer and CAR-TRP-polymer amorphous samples were subjected to a mixer mill MM 400 (Retsch GmbH & Co., Haan, Germany) placed in a cold room at approximately + 5 °C. Stainless steel jars (25 mL) with two stainless steel balls (12 mm diameter) at a milling frequency of 30 Hz were used for ball milling, and the stainless steel jars were sealed with parafilm to avoid possible moisture absorption. All samples were ball milled for various times, between 30 and 120 min (except for pure TRP that was additionally milled for 240 min). The milling process was interrupted for 5 min every 15 min to prevent the sample from overheating. After sampling, the remaining samples were continued to be milled until the end of the experiment. The samples were collected in the cold room after the ball mill jar had cooled, and stored in a desiccator over P₂O₅ at – 20 °C for further studies.

For the preparation of single amorphous components, 1000 mg of raw material powder (CAR, TRP or polymer) was weighed and

Table 2
Densities of amorphous CAR, amorphous TRP, HPMC and PVPVA64.

Samples	amorphous CAR	amorphous TRP	HPMC	PVPVA64
ρ (g/cm ³)	1.24 (Planinšek et al., 2011)	1.282	1.285 (Liu et al., 2020a)	1.285 (Guo et al., 2014b)

transferred to the milling jars. For CAR-TRP binary system, 1000 mg of the physical mixture (PM) at a CAR to TRP molar ratio of 1:1 was weighed and transferred to the jars. For CAR-polymer and TRP-polymer binary systems, the amount of polymer was 10% (w/w) of the total solid content (CAR or TRP). For CAR-TRP-polymer ternary systems, the molar ratio of CAR to TRP in the ternary system was maintained at 1:1 and the amount of polymer was 10% (w/w) of the total solid content. The

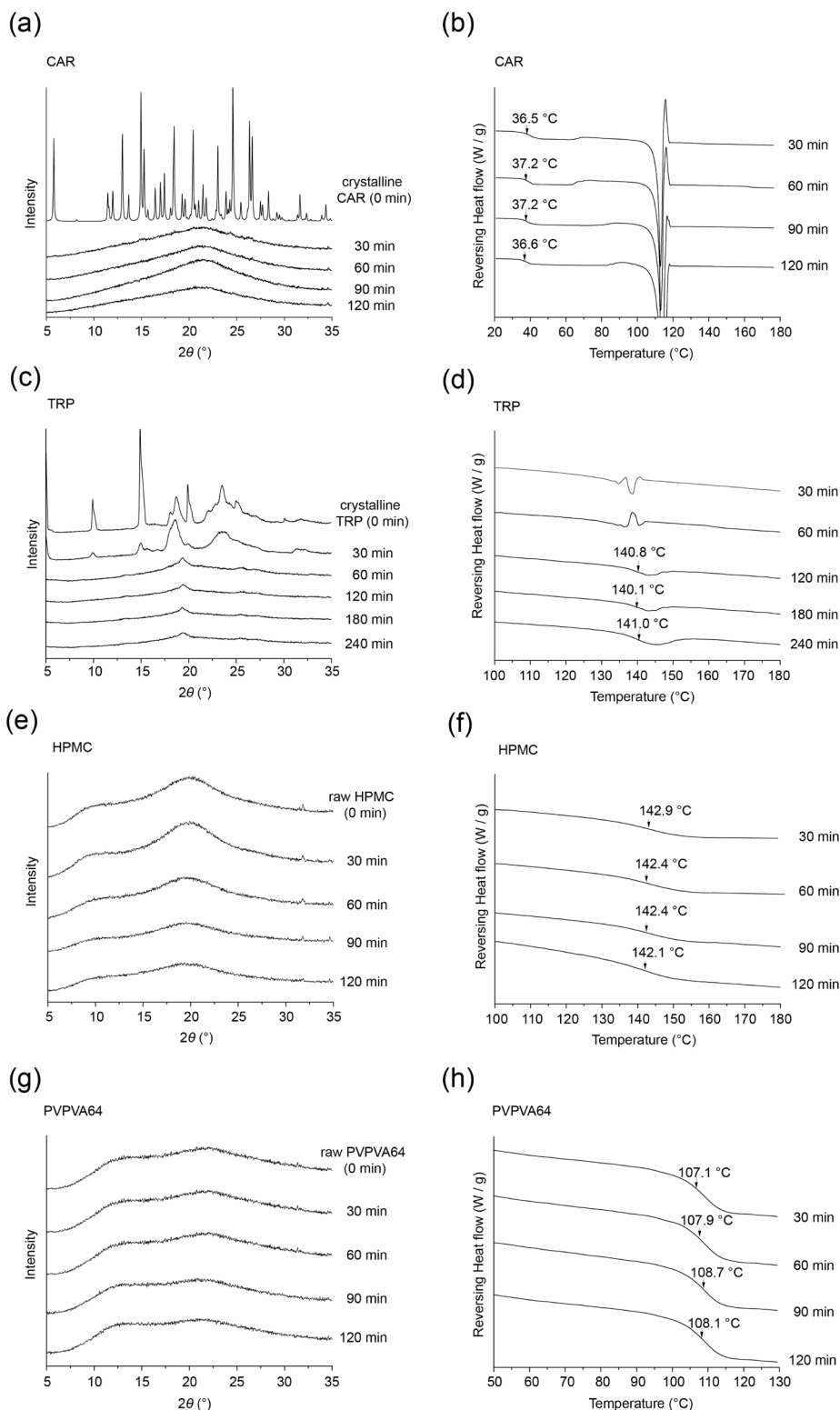


Fig. 1. XRPD diffractograms and DSC thermograms for CAR (a, b), TRP (c, d), HPMC (e, f) and PVPVA64 (g, h) after ball milling. The T_g s are indicated by arrows.

Table 3

T_g s of ball-milled single component amorphous samples ($n = 3$ for TRP, and $n = 4$ for the other groups).

Samples	CAR	TRP	HPMC	PVPVA64
$T_g \pm$ standard deviation ($^{\circ}\text{C}$)	36.9 ± 0.4	140.6 ± 0.4	142.4 ± 0.3	107.9 ± 0.7

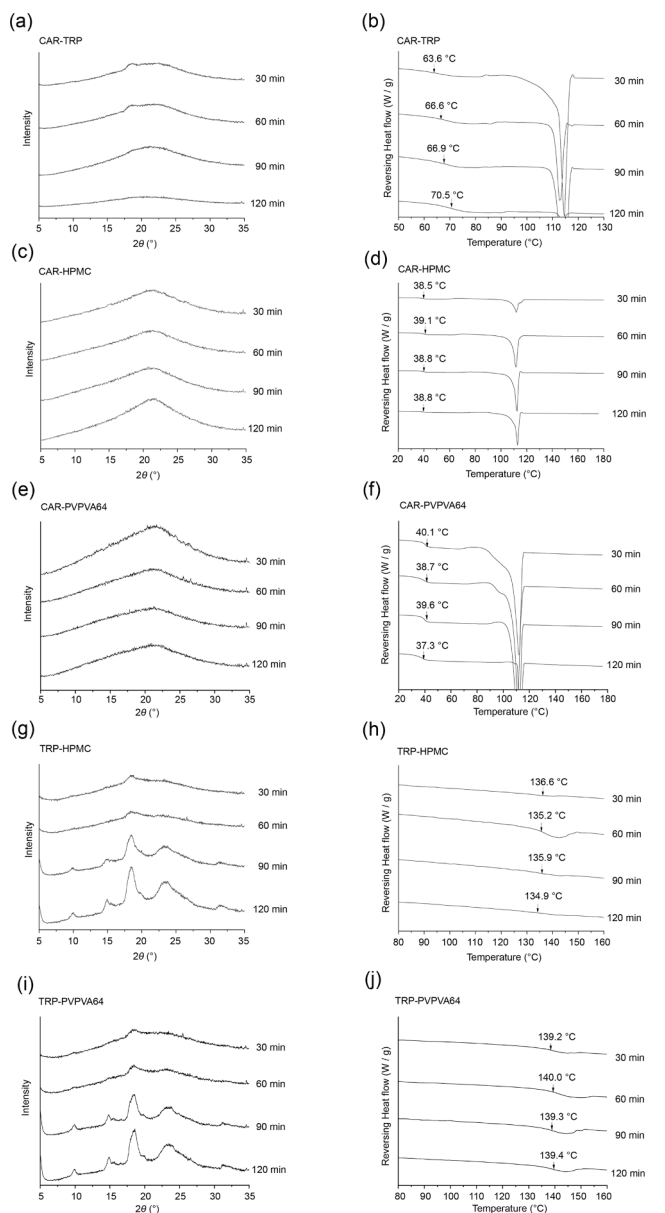


Fig. 2. XRPD diffractograms and DSC thermograms of CAR-TRP (a, b), CAR-HPMC (c, d), CAR-PVPVA64 (e, f), TRP-HPMC (g, h) and TRP-PVPVA64 (i, j) binary samples after ball milling for 30 min, 60 min, 90 min and 120 min. The T_g s are indicated by arrows.

various compositions of the physical mixtures used to prepare the single, binary and ternary system samples are shown in Table 1 (Group a).

2.2.2. Characterization of solid-state properties by x-ray powder diffraction (XRPD)

The solid-state of the samples was characterized using an X'Pert PANalytical PRO x-ray diffractometer (PANalytical, Almelo, The Netherlands), using Cu K α radiation (1.54187 Å) and an acceleration

voltage and current of 45 kV and 40 mA, respectively. The samples were placed on a plate and scanned from 5° to 35° 2 θ in reflection mode, with a scan rate and step size of 0.0625° 2 θ /s and 0.026° 2 θ , respectively. Bragg-Brentano focusing geometry was used. The data was collected and analyzed using the software X'Pert Data Collector (PANalytical, Almelo, The Netherlands).

2.2.3. Determination of the glass transition temperature by differential scanning calorimetry (DSC)

The glass transition temperature (T_g) of the various samples was determined using a Discovery DSC (TA Instruments, New Castle, DE, USA) with a 50 mL/min nitrogen gas flow. Sample powder of 3–5 mg was accurately weighed into Tzero pans and sealed with hermetic lids with a pinhole. Modulated DSC was used for the measurements. The samples were kept isothermal at -20.00°C for 5 min before being heated up to 180.00°C at an average rate of $3.00^{\circ}\text{C}/\text{min}$, with an amplitude of 0.2120°C and period 40 s. Data were collected and analyzed by the Trios software, version 5.0.0.44608 (TA Instruments, New Castle, DE, USA). The T_g was determined from the reversing heat flow signal, whilst recrystallization and melting events were observed from the total heat flow signal.

2.2.4. Calculation of the theoretical T_g s using the Gordon-Taylor equation

Theoretical T_g s were calculated for binary co-amorphous systems using the Gordon-Taylor equation:

$$T_{g12} = (\omega_1 \times T_{g1} + K \times \omega_2 \times T_{g2}) / (\omega_1 \times T_{g1} + K \times \omega_2 \times T_{g2}) \quad (1)$$

where T_{g12} and T_{gi} are the T_g s of the co-amorphous samples and the component i , respectively. ω_i is the mass fraction of the component i . K is a constant and can be calculated from the equation:

$$K = (T_{g1} \times \rho_1) / (T_{g2} \times \rho_2) \quad (2)$$

where ρ_1 and ρ_2 are the densities of the two components. No information for the density of amorphous TRP was available in the literature, and therefore was estimated by the following equation:

$$\rho_{\text{amorphousTRP}} = (\rho_{\text{amorphousCAR}} / \rho_{\text{crystallineCAR}}) \times \rho_{\text{crystallineTRP}} \quad (3)$$

where $\rho_{\text{crystalline CAR}} = 1.26 \text{ g}/\text{cm}^3$ (Planinsek et al., 2011) and $\rho_{\text{crystalline TRP}} = 1.30 \text{ g}/\text{cm}^3$ (Berlin and Pallansch, 1968). The densities of amorphous CAR, TRP, HPMC and PVPVA64 are shown in Table 2 below.

2.2.5. Investigation of intermolecular interactions by Fourier-transform infrared spectroscopy (FT-IR)

FT-IR spectra were collected using a Bomem FT-IR spectrometer (MB-Series, ABB Bomem Inc., Quebec, QC, Canada). Samples were scanned 64 times at a wavenumber range from 400 to 4000 cm^{-1} with a resolution of 4 cm^{-1} . Data was collected by GRAMS/AI software (version 7.0, Thermo Fisher Scientific, Waltham, MA, USA) and analyzed using Origin software (version 9.6.0.172, OriginLab Corporation, Northampton, MA, USA).

2.2.6. Non-sink powder dissolution testing

In order to investigate the influence of polymer on the dissolution behaviour of the drug, CAR-TRP-polymer (10% w/w) ternary co-amorphous systems with CAR to TRP molar ratios of 1:1 and 1.38:1 were prepared by ball milling and compared with single components and binary co-amorphous systems. In the CAR-TRP 1:1-polymer (10% w/w) system, the CAR content is 60.5%. Therefore, additionally the CAR-TRP 1.38:1-polymer (10% w/w) was prepared. This system contains 66.5% CAR, as do the systems with either only TRP or polymer, enabling the investigation of the dissolution behaviour at the same drug concentration, before and after addition of polymer. The different compositions and ratios of all the non-sink powder dissolution samples are shown in Table 1 (Group b).

In the non-sink powder dissolution study, a scaled-down USP2

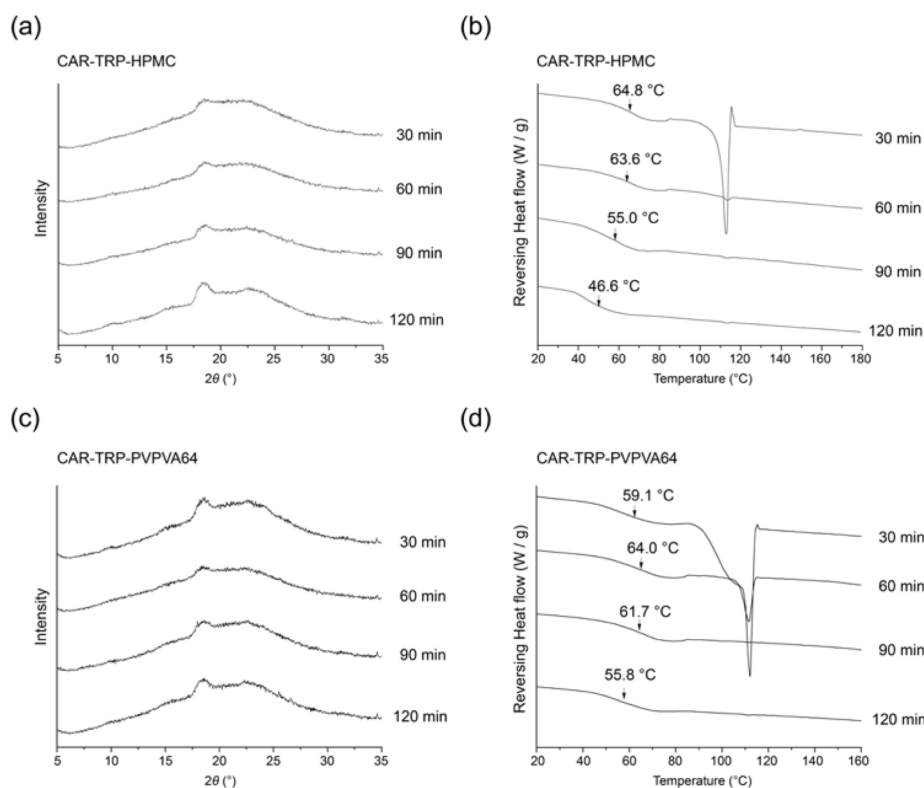


Fig. 3. XRPD diffractograms and DSC thermograms of ball milled CAR-TRP-HPMC (a, b), CAR-TRP-PVPVA64 (c, d) ternary system samples. The T_g s are indicated by arrows.

Table 4

Overview of the important stretch vibrations of the pure substances that can be affected by hydrogen bonding.

Substance	Wave number (cm ⁻¹)	Function	Type
Carvedilol	3340	N-H	Donor (Prado et al., 2014; Sadr and Nabipour, 2013)
	1249	R-O-R	Acceptor (Prado et al., 2014)
Tryptophan	3402	indole N-H	Donor (Sadhavivam et al., 2016; Sun et al., 2008)
	3463	R1-CH(R ₂)-OH (secondary alcohols)	Donor (Akinosho et al., 2013; Panini et al., 2019)
HPMC	1049	R-O-CH ₃ (methoxy groups)	Acceptor (Panini et al., 2019)
	1659	O = C (amide)	Acceptor (Chan et al., 2015; de Alencar Danda et al., 2019; Panini et al., 2019)
PVPVA64	1732	O = C (ester)	Acceptor (Chan et al., 2015; de Alencar Danda et al., 2019; Panini et al., 2019)

apparatus was used, which consisted of a set of 250 mL mini glass vessels with rotating mini paddles. A volume of 100 mL of 0.1 M phosphate buffer (pH 6.8, 37 °C) was used as the dissolution medium and the rotation speed of the mini paddles was set to 100 rpm. Powder containing a total of 100 mg CAR was added to each vessel. At pre-determined time points (1, 3, 5, 10, 15, 30, 60, 90, 120, 180, 240 and 360 min), samples of 5 mL were withdrawn and immediately replaced with the same volume of pre-warmed dissolution medium. The obtained samples were quantified by UV spectroscopy at 241.5 nm after filtration (0.45 μm filter) (Shete et al., 2012; Swamy et al., 2010). All experiments were conducted in triplicate. Afterwards, the areas under the dissolution

curves (AUCs) of all samples were calculated and compared with the AUC of crystalline CAR. One-way ANOVA and Tukey's post hoc test were performed on the AUCs to determine statistical differences ($p < 0.05$) using Prism 8.0.2 (GraphPad Software, Inc, California, USA).

2.2.7. Physical stability testing

To investigate the effects of addition of polymer on the physical stability of the non-strong interacting binary co-amorphous system CAR-TRP, a series of CAR-TRP 1:1-polymer ternary co-amorphous systems with different polymer concentrations (1%, 2%, 3%, 4%, 5% and 10% w/w) was prepared by ball milling. The different component ratios of all stability study samples are shown in Table 1 (Group c). All samples were placed in a desiccator under dry conditions. The dry conditions in the desiccator were obtained at room temperature using P₂O₅. Samples were regularly analyzed by XRPD (weekly for the first month, and every two weeks thereafter) to detect any potential re-crystallization.

3. Results and discussion

3.1. Solid state characterization

3.1.1. Preparation and characterizations of single component amorphous systems

Initially, it was determined whether the pure components became amorphous by ball milling. The XRPD diffractograms and DSC thermograms of the single components CAR, TRP, HPMC and PVPVA64 after different ball milling times are shown in Fig. 1. Neat crystalline CAR was fully amorphous after 60 min of ball milling, as shown by the lack of Bragg peaks in the XRPD diffractograms. Crystalline TRP, however, showed residual crystallinity even after 240 min of ball milling, confirming the results of a previous study (Kissi et al., 2018). HPMC and PVPVA64 are inherently amorphous polymers and their diffractograms and thermograms did not change during the ball milling process. Only one T_g was found in the DSC thermograms for each amorphous sample,

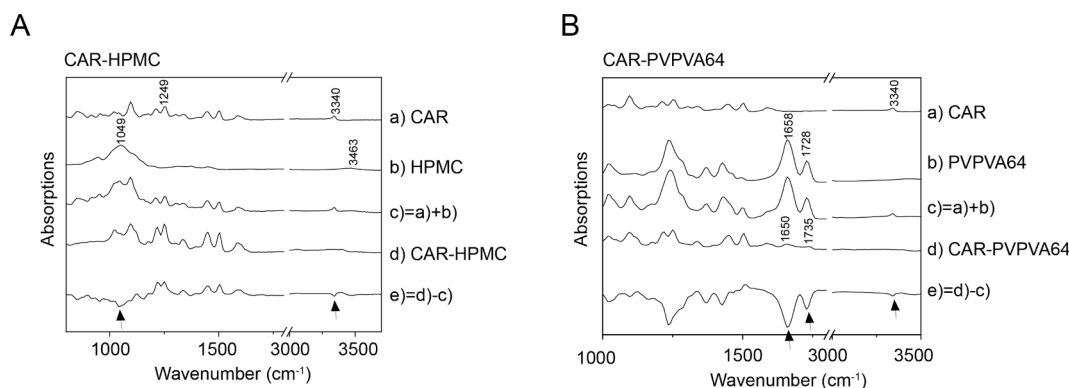


Fig. 4. FT-IR spectra of (a) amorphous CAR; (b) polymer; (c) amorphous CAR combined with polymer (addition spectrum); (d) amorphous CAR with 10% w/w polymer; (e) amorphous CAR with 10% w/w polymer (spectrum d) subtracted from amorphous CAR and polymer (spectrum c).

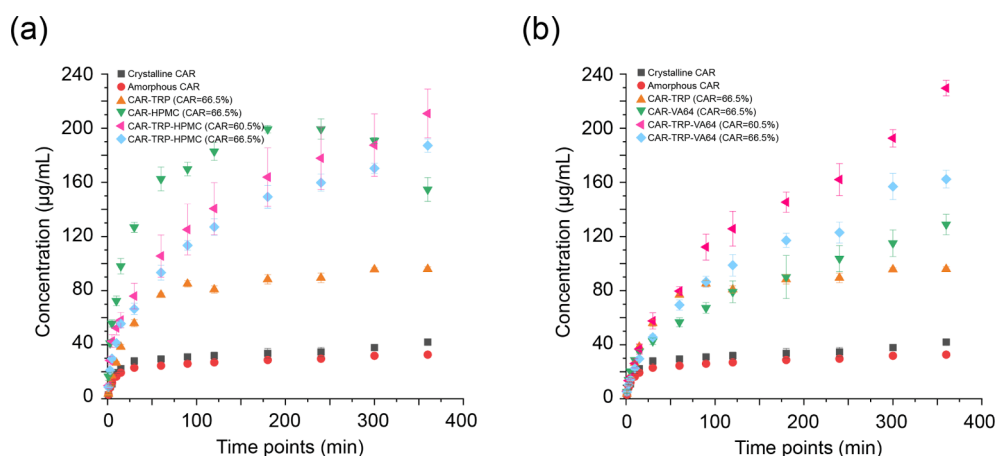


Fig. 5. Powder dissolution profiles of crystalline CAR, amorphous CAR, CAR-TRP and CAR-polymer binary co-amorphous systems and CAR-TRP-polymer ternary co-amorphous systems. (a): HPMC (b): PVPVA64.

as indicated by the arrows in the DSC thermograms in Fig. 1. The average T_g s, based on all measured time points of each single component, are shown in Table 3, and are used in the Gordon-Taylor equation in Figure S1 and S2 (supplementary materials). The T_g s are consistent with those reported in previous studies (Guo et al., 2014b; Jensen et al., 2014; Liu et al., 2020a; Liu et al., 2020b).

3.1.2. Characterizations of binary co-amorphous systems

Fig. 2 shows the XRPD diffractograms and DSC thermograms of the CAR-TRP, CAR-HPMC, CAR-PVPVA64, TRP-HPMC, and TRP-PVPVA64 binary physical mixtures, after different ball milling times. After ball milling, all samples displayed a halo in their XRPD patterns, indicating successful amorphization. However, the amorphous forms were only maintained for short times in TRP-HPMC and TRP-PVPVA64 binary systems, as some recrystallization was observed after 90 min of milling time (Fig. 2g, 2i). This recrystallisation was not observed in the DSC as the recrystallisation is attributed to TRP which possesses a melting point of around 290 °C (Yonemitsu et al., 1966).

The amorphized samples were further investigated by DSC to identify if the ball-milled binary physical mixtures formed a homogeneous single phase and to determine the respective T_g s. Only one T_g was detected in each DSC thermogram of all the ball-milled binary samples, indicating the formation of co-amorphous systems. During the ball milling process, the T_g positions did not change with time in CAR-HPMC, TRP-HPMC, CAR-PVPVA64 and TRP-PVPVA64 binary co-amorphous systems, while the T_g s of CAR-TRP binary systems varied from approx. 63.6 °C to approx. 70.5 °C with increasing milling time. The data shows that, upon milling, the T_g is slightly increasing and thus that the

amorphization kinetics for the two components are not exactly the same, but that the component with the lower T_g (CAR) is amorphized slightly faster than TRP, and thus that the resulting co-amorphous mixtures over time increase in TRP content until fully co-amorphous. This may affect physical stability and will be discussed in more detail in section 3.4.

In order to investigate the molecular interactions in CAR containing binary co-amorphous systems, additional CAR-TRP and CAR-polymer ball-milled systems with different drug weight fractions ranging from 10% to 90% were prepared by ball milling for 60 min and characterized by DSC and by employing the Gordon-Taylor equation. The measured T_g s of these CAR containing binary co-amorphous systems are shown in the supporting information (the DSC thermograms for CAR-TRP and CAR-polymer systems with different drug weight fractions are shown in Figure S1(a) and Figure S2 (a) and (c), respectively). No strong interactions were observed in CAR-TRP binary co-amorphous systems (which would have shown as deviations of the T_g from the T_g s predicted by the Gordon-Taylor equation (Di et al., 2021; Jensen et al., 2014)), while drug-polymer interactions were clearly detectable in CAR-polymer binary amorphous system (deviations of the T_g from the T_g s predicted by the Gordon-Taylor equation), indicating that the molecular interactions between CAR and polymer are stronger than those between CAR and TRP.

3.1.3. Preparation and characterizations of ternary co-amorphous systems

The XRPD diffractograms and DSC thermograms of the two ternary physical mixtures, CAR-TRP-HPMC and CAR-TRP-PVPVA64, after 30, 60, 90 and 120 min of ball milling are shown in Fig. 3. The DSC thermograms of the ball-milled ternary physical mixtures are shown in

Table 5

C_{max} , T_{max} and the areas under dissolution curves after the powder dissolution studies.

	CAR content (w/w)	Areas under dissolution curves (min- $\mu\text{g}/\text{mL}$) (0–360 min)*	Relative percentage of areas under dissolution curves (%)	C_{max} ($\mu\text{g}/\text{mL}$)	T_{max} (min)
Crystalline CAR	100.0%	11887 \pm 868 _{a,b,c}	100%	42 \pm 2	360
Amorphous CAR	100.0%	9959 \pm 179 _{a,b,c}	84%	33 \pm 1	360
CAR-TRP 1:1	66.5%	29632 \pm 660	249%	96 \pm 2	360
CAR(66.5% w/w)-HPMC	66.5%	62678 \pm 472	527%	199 \pm 2	180
CAR-TRP 1.38:1-HPMC	66.5%	48701 \pm 2418 ^b	410%	187 \pm 5	360
CAR-TRP 1:1-HPMC (10% w/w)	60.5%	54081 \pm 11159 ^{a,b}	455%	211 \pm 18	360
CAR(66.5% w/w)-PVPVA64	66.5%	31221 \pm 2664	263%	129 \pm 8	360
CAR-TRP 1.38:1-PVPVA64	66.5%	39314 \pm 1709 ^c	331%	129 \pm 8	360
CAR-TRP 1:1-PVPVA64 (10% w/w)	60.5%	50182 \pm 2306 ^{a,c}	422%	162 \pm 7	360

The percentage in parenthesis stands for added polymer relative to other ingredients.

* Superscripts a, b, c indicate statistically significant differences at levels $p = 0.0086$, $p = 0.0096$ and $p = 0.0001$ respectively. Mean \pm standard deviation, $n = 3$.

Fig. 3b and 3d. The presence of only a single T_g indicates that the amorphized CAR-TRP-polymer ternary samples formed single-phase homogeneous co-amorphous phases. It should be noted that the changing trends in the T_g positions in the thermograms in CAR-TRP-polymer ternary co-amorphous systems with HPMC and PVPVA64 are different from those in CAR-TRP binary co-amorphous systems (as shown in Fig. 2b). A decrease in T_g s was found for both ternary co-amorphous systems as the ball milling time increased, whilst an increase in T_g s occurred in the binary co-amorphous systems during ball milling. In addition, no endothermic peak can be detected in the DSC thermograms in Fig. 3b and 3d upon milling for 60 min or longer, indicating that no melting event of crystalline CAR occurred. The total heat flow of amorphous CAR, CAR-TRP binary co-amorphous system and CAR-TRP-polymer (10% w/w) ternary systems are shown in

Figure S3, indicating that the melting event of crystalline CAR is due to recrystallization of CAR during heating. Therefore, compared with the binary co-amorphous systems, the addition of polymer inhibited the recrystallization of CAR and influenced the changing trends in the T_g s upon heating.

3.2. Investigation of intermolecular interaction in the co-amorphous systems by FT- IR

In order to investigate the type of molecular interactions between CAR-TRP and CAR-polymer in the ternary co-amorphous systems, FT-IR studies were performed. CAR has one hydrogen bond donor group (N-H group) along with one acceptor R-O-R group (C-O stretching vibration of ether groups) in the molecule; TRP has a polar N-H group that can donate a hydrogen bond; HPMC has donor hydrogen bonds (–OH groups) along with proton acceptor oxygens, from the methoxy groups in the molecule; PVPVA64 has two potential proton acceptor functional groups (O = C as amide and ester group). Theoretically, various interactions can be formed due to different kinds of potential donor–acceptor combinations.

A high degree of similarity of the amorphous CAR vibrations with those found in CAR-TRP systems has previously been described suggesting that the compounds in these co-amorphous blends had no specific or strong interactions with each other (Di et al., 2021). This is also supported by the lack of deviation of the experimentally determined T_g values from those calculated using the Gordon-Taylor equation of various CAR-TRP systems (shown in the supporting information, Figure S1(b)).

For CAR-polymer systems, in order to determine which functional groups form hydrogen bonds between CAR and polymer, the FT-IR spectra of single components (CAR and polymer) and binary co-amorphous samples (CAR-polymer) were determined, and were used as control samples aiding the interpretation of the spectra of the ternary co-amorphous systems.

An overview of the important stretch vibrations of CAR, TRP, HPMC and PVPVA64 that can be affected by hydrogen bonding is given in Table 4.

3.2.1. Intermolecular interactions between CAR and polymer

Pure amorphous CAR shows characteristic peaks at 3340 cm^{-1} (N-H stretching vibration (Prado et al., 2014)) and 1249 cm^{-1} (R-O stretching vibration (Prado et al., 2014)). The most intense peak of HPMC in the spectra occurred at 1049 cm^{-1} (out-of-phase vibration associated with an alkyl substituted cyclic ring containing ether linkages (Panini et al., 2019)) and 3463 cm^{-1} (C-O bonds involved in methoxy groups (Panini et al., 2019)). PVPVA64 showed two characteristic peaks at 1659 cm^{-1} and 1732 cm^{-1} (C = O stretching vibrations of carbonyl group (Chan et al., 2015)). The spectra of pure amorphous CAR (Fig. 4a) and polymer

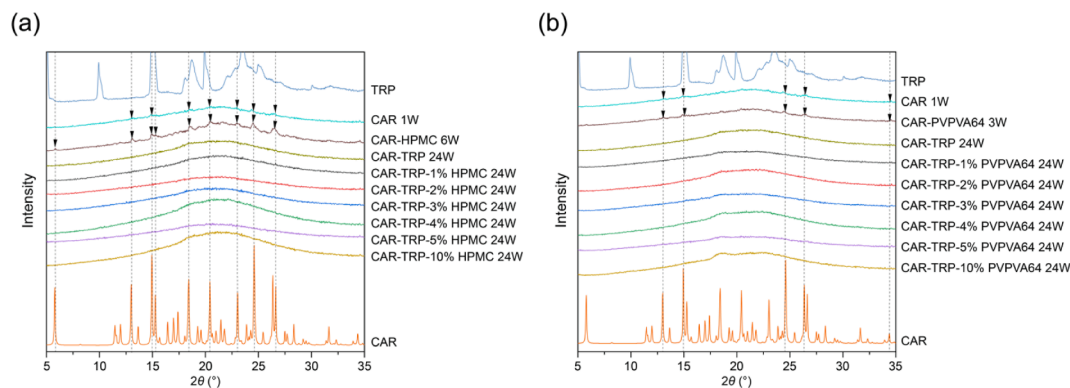


Fig. 6. XRPD diffractograms of various amorphous systems stored at room temperature, dry condition. The arrows show peaks after recrystallization. W = weeks of storage stated in the figure legends.

(Fig. 4b) were combined at equal weighting to obtain the combination spectrum (Fig. 4c). Subtraction of the CAR-polymer system sample spectrum (Fig. 4d) from the combination spectrum resulted in the FT-IR difference spectrum (Fig. 4e). The combination spectrum shows the amorphous mixture without interactions while the FT-IR difference spectra show the possible interactions in the co-amorphous sample.

When comparing the FT-IR difference spectra with the spectra of amorphous CAR and polymer, in CAR-HPMC co-amorphous systems, the N-H stretching vibration peaks of CAR and R-O-CH₃ characteristic peaks of HPMC disappeared, whilst in the CAR-PVPVA64 co-amorphous system, the N-H stretching vibration peaks of CAR and C = O in PVPVA64 disappeared. This result shows that hydrogen bonds are formed between N-H in CAR and C-O in HPMC and C = O in PVPVA64, respectively, and that CAR is the hydrogen bond donor (Oh et al., 2011; Shim et al., 2012). Therefore, compared with the non-strongly interacting binary co-amorphous CAR-TRP, a stronger hydrogen bond is formed between CAR and polymer in the ternary co-amorphous CAR-TRP-polymer system.⁴

3.3. Powder dissolution of single component, binary and ternary systems

A non-sink powder dissolution study was performed to evaluate the possibilities of dissolution enhancement of the different (co-)amorphous systems with polymer. The dissolution behaviours of crystalline CAR, amorphous CAR, CAR-TRP and CAR-polymer binary systems (66.5% CAR) and CAR-TRP-polymer ternary systems (60.5% and 66.5% CAR) are shown in Fig. 5 and the C_{max} , T_{max} and areas under dissolution curves after the powder dissolution studies are shown in Table 5.

The dissolved drug concentration of crystalline CAR was detected to be $42 \pm 2 \mu\text{g/mL}$ in the dissolution medium after 6 h, which corresponded to a previously reported saturation solubility study (Hamed et al., 2016). The dissolved drug concentration of amorphous CAR was about 84% of the crystalline form at the end of dissolution testing, which is also consistent with a previous report (Liu et al., 2020a) and can be explained by undissolved amorphous CAR converting to the crystalline form upon contact with the dissolution medium (Planinšek et al., 2011; Pokharkar et al., 2006).

An over two-fold higher dissolved drug concentration was observed for the CAR-TRP systems compared to that of the crystalline CAR. The CAR-HPMC and CAR-PVPVA64 binary systems showed a significantly higher initial drug release rate for the first 3 h and achieved supersaturation compared with the neat crystalline CAR, however, this supersaturation was followed by precipitation for the CAR-HPMC system.

For the CAR-TRP-HPMC ternary systems with different component ratios, a larger area under the dissolution curve was observed compared with the CAR-TRP binary systems, which can be regarded as an improvement in dissolution behaviour. Compared with the CAR-HPMC binary system, the time of a maintained high-level saturation is longer and the dissolved drug concentration was more than four-fold higher compared to that of the crystalline and amorphous pure drug. As was the case for the CAR-TRP-HPMC ternary system, the CAR-TRP-PVPVA64 ternary system also improved the dissolution behaviour, but PVPVA64 was not as effective as HPMC in improving solubility. The high level of saturation was maintained for a longer period. This might have been caused by the addition of the polymer reducing the recrystallization tendency of CAR (Figs. 3 and S3). This improvement of dissolution behaviour (both dissolution rate and apparent solubility) might thus be reflected in the thermal behaviour of the systems. The CAR-TRP system recrystallized upon heating whereas the ternary systems did not. Interestingly, in both ternary systems, the samples with lower drug concentration (60.5% CAR) show a slightly higher solubility at each time point than the samples with higher drug concentration (66.5% CAR), indicating the importance of drug to excipient ratio in the ternary systems on the dissolution behaviour of the drug.

3.4. Physical stability of single component, binary and ternary systems

The physical stability of single component (amorphous CAR), binary co-amorphous systems (CAR-TRP 1:1 and CAR-polymer (10% w/w)) and ternary co-amorphous systems (CAR-TRP 1:1-polymer with different polymer content) was investigated upon storage at room temperature under dry conditions (Fig. 6). Within the 6 months study period, binary co-amorphous CAR-TRP and all of the CAR-TRP-polymer ternary systems remained amorphous. In contrast, pure amorphous CAR and amorphous CAR-PVPVA64 and CAR-HPMC, recrystallized after one week, three weeks, and six weeks of storage, respectively. Therefore, it can be concluded that the binary co-amorphous systems CAR-TRP and CAR-polymer are more stable than the pure amorphous CAR and that the addition of polymer did not negatively effect the physical stability of the non-strongly interacting co-amorphous systems CAR-TRP.

4. Conclusion

In this study, the effects of polymer addition (HPMC and PVPVA64) on the physical properties (amorphization, dissolution and physical stability) of the non-strongly interacting binary co-amorphous system CAR-TRP (1:1 mol/mol) were investigated. Homogeneous CAR-TRP-polymer ternary amorphous systems could be successfully prepared by ball milling. The polymer was found to be involved in molecular interactions in the CAR-TRP-polymer systems and formed hydrogen bonds between CAR and polymer. CAR-TRP-polymer ternary systems could improve the dissolution behavior by increasing the initial dissolution rate of the CAR-TRP system and maintaining supersaturation for a longer period of time. In addition, no negative effect of polymer addition on physical stability was observed at room temperature under dry conditions for 6 months. Therefore, a small amount of polymer can be added into co-amorphous binary systems to design ternary co-amorphous drug delivery systems with optimized dissolution characteristics.

Funding

This research did not receive any specific grant from funding agencies in the public, commercial, or not-for-profit sectors.

CRediT authorship contribution statement

Yixuan Wang: Methodology, Formal analysis, Investigation, Writing – original draft, Visualization. **Holger Grohganz:** Conceptualization, Writing – review & editing, Supervision, Project administration. **Thomas Rades:** Methodology, Conceptualization, Writing – review & editing, Supervision.

Declaration of Competing Interest

The authors declare that they have no known competing financial interests or personal relationships that could have appeared to influence the work reported in this paper.

Appendix A. Supplementary material

Supplementary data to this article can be found online at <https://doi.org/10.1016/j.ijpharm.2022.121625>.

References

- Akinosho, H., Hawkins, S., Wicker, L., 2013. Hydroxypropyl methylcellulose substituent analysis and rheological properties. *Carbohydrate Polymers* 98 (1), 276–281.
- An, C., Zhou, Y., Chen, C., Fei, F., Song, F., Park, C., Zhou, J., Rubahn, H.-G., Moshchalkov, V.V., Chen, X., Zhang, G., Yang, Z., 2020. Long-range ordered amorphous atomic chains as building blocks of a superconducting quasi-one-

- dimensional crystal. *Advanced Materials* 32 (38), 2002352. <https://doi.org/10.1002/adma.v32.3810.1002/adma.202002352>.
- Berlin, E., Pallansch, M.J., 1968. Densities of several proteins and L-amino acids in the dry state. *The Journal of Physical Chemistry* 72 (6), 1887–1889.
- Carstensen, J.J.D.D., Pharmacy, I., 1988. Effect of moisture on the stability of solid dosage forms. *Drug Development and Industrial Pharmacy* 14, 1927–1969.
- Chan, S.-Y., Chung, Y.-Y., Cheah, X.-Z., Tan, E.-L., Quah, J., 2015. The characterization and dissolution performances of spray dried solid dispersion of ketoprofen in hydrophilic carriers. *Asian Journal of Pharmaceutical Sciences* 10 (5), 372–385.
- de Alencar Danda, L.J., de Medeiros Batista, L., Melo, V.C.S., Sobrinho, J.L.S., Soares, M. F.d.L.R., 2019. Combining amorphous solid dispersions for improved kinetic solubility of posaconazole simultaneously released from soluble PVP/VA64 and an insoluble ammonio methacrylate copolymer. *European Journal of Pharmaceutical Sciences* 133, 79–85.
- Dengale, S.J., Grohgan, H., Rades, T., Löbmann, K., 2016. Recent advances in co-amorphous drug formulations. *Advanced Drug Delivery Reviews* 100, 116–125.
- Di, R., Liu, J., Grohgan, H., Rades, T., 2021. A multivariate approach for the determination of the optimal mixing ratio of the non-strong interacting co-amorphous system carvedilol-tryptophan. *Molecules* 26 (4), 801. <https://doi.org/10.3390/molecules26040801>.
- Fucke, K., Myz, S.A., Shakhtshneider, T.P., Boldyreva, E.V., Griesser, U.J., 2012. How good are the crystallisation methods for co-crystals? A comparative study of piroxicam. *New Journal of Chemistry* 36 (10), 1969. <https://doi.org/10.1039/c2nj40093f>.
- Guo, H., Miao, N., Li, T., Hao, J., Gao, Y., Zhang, J., 2014a. Pharmaceutical coamorphous—a newly defined single-phase amorphous binary system. *Progress in Chemistry* 26, 478.
- Guo, Z., Lu, M., Li, Y., Pang, H., Lin, L., Liu, X., Wu, C., 2014b. The utilization of drug-polymer interactions for improving the chemical stability of hot-melt extruded solid dispersions. *Journal of Pharmacy and Pharmacology* 66, 285–296.
- Hamed, R., Awadallah, A., Sunoqrot, S., Tarawneh, O., Nazzal, S., AlBaragathi, T., Al Sayyad, J., Abbas, A., 2016. pH-dependent solubility and dissolution behavior of carvedilol—case example of a weakly basic BCS class II drug. *AAPS PharmSciTech* 17 (2), 418–426.
- Hancock, B.C., Zografi, G., 1997. Characteristics and significance of the amorphous state in pharmaceutical systems. *Journal of Pharmaceutical Science* 86 (1), 1–12.
- Hirani, J.J., Rathod, D.A., Vadalía, K.R., 2009. Orally disintegrating tablets: A review. *Tropical Journal of Pharmaceutical Research* 8.
- Huang, Y., Zhang, Q.i., Wang, J.-R., Lin, K.-L., Mei, X., 2017. Amino acids as co-amorphous excipients for tackling the poor aqueous solubility of valsartan. *Pharmaceutical Development and Technology* 22 (1), 69–76.
- Jensen, K., Löbmann, K., Rades, T., Grohgan, H., 2014. Improving co-amorphous drug formulations by the addition of the highly water soluble amino acid, proline. *Pharmaceutics* 6 (3), 416–435.
- Karagianni, A., Kachrimanis, K., Nikolakakis, I., 2018. Co-amorphous solid dispersions for solubility and absorption improvement of drugs: Composition, preparation, characterization and formulations for oral delivery. *Pharmaceutics* 10 (3), 98. <https://doi.org/10.3390/pharmaceutics10030098>.
- Kissi, E.O., Kasten, G., Löbmann, K., Rades, T., Grohgan, H., 2018. The role of glass transition temperatures in coamorphous drug-amino acid formulations. *Molecular Pharmaceutics* 15 (9), 4247–4256.
- Laitinen, R., Löbmann, K., Grohgan, H., Priemel, P., Strachan, C.J., Rades, T., 2017. Supersaturating drug delivery systems: The potential of co-amorphous drug formulations. *International Journal of Pharmaceutics* 532 (1), 1–12.
- Liu, J., Grohgan, H., Rades, T., 2020a. Influence of polymer addition on the amorphization, dissolution and physical stability of co-amorphous systems. *International Journal of Pharmaceutics* 588, 119768. <https://doi.org/10.1016/j.ijpharm.2020.119768>.
- Liu, J., Rades, T., Grohgan, H., 2020b. Determination of the optimal molar ratio in amino acid-based coamorphous systems. *Molecular Pharmaceutics* 17 (4), 1335–1342.
- Löbmann, K., Strachan, C., Grohgan, H., Rades, T., Korhonen, O., Laitinen, R., 2012. Co-amorphous simvastatin and glipizide combinations show improved physical stability without evidence of intermolecular interactions. *European Journal of Pharmaceutics and Biopharmaceutics* 81 (1), 159–169.
- Oh, M.-J., Shim, J.-B., Lee, E.-Y., Yoo, H.-N., Cho, W.-H., Lim, D.-K., Lee, D.-W., Khang, G.-S., 2011. Molecular effect of PVP on the release property of carvedilol solid dispersion. *Journal of Pharmaceutical Investigation* 41 (3), 179–184.
- Panini, P., Rampazzo, M., Singh, A., Vanhoutte, F., Van den Mooter, G., 2019. Myth or truth: The glass forming ability class III drugs will always form single-phase homogenous amorphous solid dispersion formulations. *Pharmaceutics* 11 (10), 529. <https://doi.org/10.3390/pharmaceutics11100529>.
- Planinšek, O., Kovačić, B., Vrečer, F., 2011. Carvedilol dissolution improvement by preparation of solid dispersions with porous silica. *International Journal of Pharmaceutics* 406 (1-2), 41–48.
- Pokharkar, V.B., Mandpe, L.P., Padamwar, M.N., Ambike, A.A., Mahadik, K.R., Paradkar, A., 2006. Development, characterization and stabilization of amorphous form of a low Tg drug. *Powder Technology* 167 (1), 20–25.
- Prado, L.D., Rocha, H.V.A., Resende, J.A.L.C., Ferreira, G.B., de Figureido Teixeira, A.M. R., 2014. An insight into carvedilol solid forms: Effect of supramolecular interactions on the dissolution profiles. *CrystEngComm* 16 (15), 3168–3179.
- Sadhasivam, B., Muthusamy, S., 2016. Thermal and dielectric properties of newly developed L-tryptophan-based optically active polyimide and its POSS nanocomposites. *Designed Monomers and Polymers* 19 (3), 236–247.
- Sadr, M.H., Nabipour, H., 2013. Synthesis and identification of carvedilol nanoparticles by ultrasound method. *Journal of Nanostructure in Chemistry* 3, 26.
- Shete, A.S., Yadav, A.V., Murthy, S.M., 2012. Chitosan and chitosan chlorhydrate based various approaches for enhancement of dissolution rate of carvedilol. *DARU Journal of Pharmaceutical Sciences* 20, 1–9.
- Shim, J.B., Kim, M.J., Kim, S.J., Kang, S.J., Lee, J.H., Kim, H.S., Lee, D., Khang, G., 2012. Dissolution properties of control released solid dispersion of carvedilol with HPMC and Eudragit RS. *Journal of Pharmaceutical Investigation* 42 (5), 285–291.
- Sun, H., Greathouse, D.V., Andersen, O.S., Koeppe, R.E., 2008. The preference of tryptophan for membrane interfaces insights from n-methylation of tryptophans in gramicidin channels. *Journal of Biological Chemistry* 283 (32), 22233–22243.
- Swamy, P., Shilpa, H., Shirsand, S., Gada, S., Kinagi, M., 2010. Role of cogrinding in enhancing the in vitro dissolution characteristics of carvedilol. *International journal of pharmaceutical sciences research* 1, 232–237.
- Tang, B.o., Cheng, G., Gu, J.-C., Xu, C.-H., 2008. Development of solid self-emulsifying drug delivery systems: preparation techniques and dosage forms. *Drug Discovery Today* 13 (13-14), 606–612.
- Țița, B., Fuliș, A., Bandur, G., Marian, E., Țița, D., 2011. Compatibility study between ketoprofen and pharmaceutical excipients used in solid dosage forms. *Journal of Pharmaceutical Biomedical Analysis* 56 (2), 221–227.
- Warren, D.B., Benameur, H., Porter, C.J.H., Pouton, C.W., 2010. Using polymeric precipitation inhibitors to improve the absorption of poorly water-soluble drugs: A mechanistic basis for utility. *Journal of Drug Targeting* 18 (10), 704–731.
- Wei, Y., Ling, Y., Su, M., Qin, L., Zhang, J., Gao, Y., Qian, S., 2018. Characterization and stability of amorphous tadalafil and four crystalline polymorphs. *Chemical and Pharmaceutical Bulletin* 66 (12), 1114–1121.
- Wu, W., Wang, Y., Löbmann, K., Grohgan, H., Rades, T., 2019. Transformations between co-amorphous and co-crystal systems and their influence on the formation and physical stability of co-amorphous systems. *Molecular Pharmaceutics* 16 (3), 1294–1304.
- Xie, T., Gao, W., Taylor, L.S., 2017. Impact of Eudragit EPO and hydroxypropyl methylcellulose on drug release rate, supersaturation, precipitation outcome and redissolution rate of indomethacin amorphous solid dispersions. *International Journal of Pharmaceutics* 531 (1), 313–323.
- Yonemitsu, O., Cerutti, P., Witkop, B., 1966. Photoreductions and photocyclizations of tryptophan. *Journal of the American Chemical Society* 88 (17), 3941–3945.